



# ATLAS/ICESat-2 L3A Land Ice Height, Version 6

---

## USER GUIDE

### How to Cite These Data

As a condition of using these data, you must include a citation:

Smith, B., S. Adusumilli, B. M. Csathó, D. Felikson, H. A. Fricker, A. Gardner, N. Holschuh, J. Lee, F. S. Paolo, M. R. Siegfried, T. Sutterley and the ICESat-2 Science Team. 2023. *ATLAS/ICESat-2 L3A Land Ice Height, Version 6*. [Indicate subset used]. Boulder, Colorado USA. NASA National Snow and Ice Data Center Distributed Active Archive Center. <https://doi.org/10.5067/ATLAS/ATL06.006>. [Date Accessed].

FOR QUESTIONS ABOUT THESE DATA, CONTACT [NSIDC@NSIDC.ORG](mailto:NSIDC@NSIDC.ORG)

FOR CURRENT INFORMATION, VISIT <https://nsidc.org/data/ATL06>



National Snow and Ice Data Center

# TABLE OF CONTENTS

1	DATA DESCRIPTION .....	2
1.1	Parameters .....	2
1.2	File Information .....	2
1.2.1	Format .....	2
1.2.2	ATLAS/ICESat-2 Description .....	2
1.2.3	File Contents .....	6
1.2.4	Data Groups .....	7
1.2.5	Naming Convention .....	9
1.3	Spatial Information .....	10
1.3.1	Coverage .....	10
1.3.2	Resolution .....	10
1.3.3	Geolocation .....	10
1.4	Temporal Information .....	11
1.4.1	Coverage .....	11
1.4.2	Resolution .....	11
2	DATA ACQUISITION AND PROCESSING .....	11
2.1	Background .....	11
2.2	Acquisition .....	12
2.3	Processing .....	13
2.4	Quality, Errors, and Limitations .....	14
3	VERSION HISTORY .....	15
4	REFERENCES .....	15
4.1	References .....	15
5	DOCUMENT INFORMATION .....	16
5.1	Publication Date .....	16
5.2	Date Last Updated .....	16

# 1 DATA DESCRIPTION

## 1.1 Parameters

---

Geolocated land-ice surface heights (above the WGS 84 ellipsoid, ITRF2014 reference frame), plus ancillary parameters that can be used to interpret and assess the quality of the height estimates.

## 1.2 File Information

---

### 1.2.1 Format

Data are provided as HDF5 formatted files.

### 1.2.2 ATLAS/ICESat-2 Description

Note: The following brief description of the Ice, Cloud and land Elevation Satellite-2 (ICESat-2) observatory and Advanced Topographic Laser Altimeter System (ATLAS) instrument is provided to help users better understand the file naming conventions, internal structure of data files, and other details referenced by this user guide. The ATL06 data product is described in detail in the Ice, Cloud, and land Elevation Satellite-2 Project Algorithm Theoretical Basis Document for Land-Ice Along-Track Products (ATL06 ATBD | V6, <https://doi.org/10.5067/VWOKQDYJ7ODB>).

The ICESat-2 observatory utilizes a photon-counting lidar (the ATLAS instrument) and ancillary systems (GPS, star cameras, and ground processing) to measure the time a photon takes to travel from ATLAS to Earth and back again and determine the reflected photon's geodetic latitude and longitude. Laser pulses from ATLAS illuminate three left/right pairs of spots on the surface that trace out six approximately 14 m wide ground tracks as ICESat-2 orbits Earth. Each ground track is numbered according to the laser spot number that generates it, with ground track 1L (GT1L) on the far left and ground track 3R (GT3R) on the far right. Left/right spots within each pair are approximately 90 m apart in the across-track direction and 2.5 km in the along-track direction. Higher level ATLAS/ICESat-2 data products (ATL03 and above) are organized by ground track, with ground tracks 1L and 1R forming pair one, ground tracks 2L and 2R forming pair two, and ground tracks 3L and 3R forming pair three. Each pair also has a Pair Track—an imaginary line halfway between the actual location of the left and right beams (see Figure 1). Pair tracks are approximately 3 km apart in the across-track direction.

The beams within each pair have different transmit energies—so-called weak and strong beams—with an energy ratio between them of approximately 1:4. The mapping between the strong and weak beams of ATLAS, and their relative position on the ground, depends on the orientation (yaw)

of the ICESat-2 observatory, which is changed approximately twice per year to maximize solar illumination of the solar panels. The forward orientation corresponds to ATLAS traveling along the +x coordinate in the ATLAS instrument reference frame (see Figure 1, left). In this orientation, the weak beams lead the strong beams and a weak beam is on the left edge of the beam pattern. In the backward orientation, ATLAS travels along the -x coordinate, in the instrument reference frame, with the strong beams leading the weak beams and a strong beam on the left edge of the beam pattern (see Figure 1, right). The first yaw flip was performed on 28 December 2018, placing the spacecraft into the backward orientation. ATL06 reports the spacecraft orientation in the `sc_orient` parameter stored in the `/orbit_info/` data group (see section 1.2.4 Data Groups). In addition, the current spacecraft orientation, as well as a history of previous yaw flips, is available in the [ICESat-2 Major Activities](#) tracking document (.xlsx).

The Reference Ground Track (RGT) refers to the imaginary track on Earth at which a specified unit vector within the observatory is pointed. During nominal operating conditions onboard software aims the laser beams so that the RGT is between ground tracks 2L and 2R (i.e., coincident with Pair Track 2). The ICESat-2 mission acquires data along 1,387 different RGTs. Each RGT is targeted in the polar regions once every 91 days to allow elevation changes to be detected. Cycle numbers track the number of 91-day periods that have elapsed since the ICESat-2 observatory entered the science orbit. RGTs are uniquely identified, for example in ATL02 file names, by appending the two-digit cycle number (cc) to the RGT number, e.g., 0001cc to 1387cc.

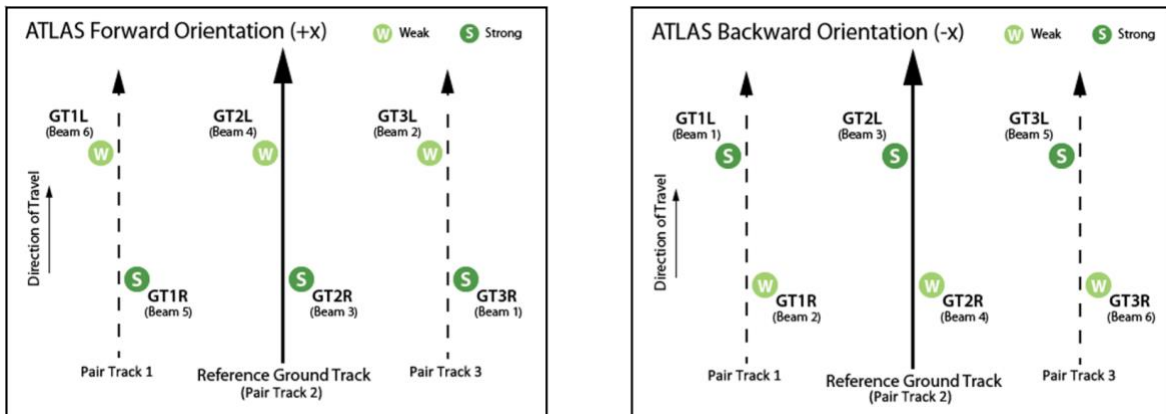


Figure 1. Spot and ground track (GT) naming convention with ATLAS oriented in the forward (instrument coordinate +x) direction and backward (instrument coordinate -x) direction.

Under normal operating conditions, no data are collected along the RGT; however, during spacecraft slews, or off-pointing, some ground tracks may intersect the RGT. Off-pointing refers to a series of plans over the mid-latitudes that have been designed to facilitate a global ground and canopy height data product with approximately 2 km track spacing. Off-pointing began on 1 August 2019 with RGT 518, after the ATLAS/ICESat-2 PPD and POD solutions had been adequately

resolved and the instrument had pointed directly at the reference ground track for at least a full 91 days (1,387 orbits).

Users should note that sometimes, for various reasons, the spacecraft pointing may lead to ICESat-2 data collected offset at some distance from the RGTs instead of along the nominal RGT. Although not along the nominal RGT, the geolocation information and data quality for these data are not degraded. As an example, from 14 October 2018 and 30 March 2019, the spacecraft pointing control was not yet optimized. To identify such time periods, refer to the ICESat-2 Major Activities file.

Note: ICESat-2 reference ground tracks with dates and times can be downloaded as KMZ files from NASA's [ICESat-2 | Technical Specs](#) page (below the Orbit and Coverage table).

Various reference systems and dynamic processes, or geophysical corrections, occur during an ATLAS/ICESat-2 measurement (Figure 2). Table 1 lists the corrections needed for each surface type and ICESat-2 product. For example, to determine an estimate of the mean sea surface, several well-modeled, time-varying effects must be accounted for.

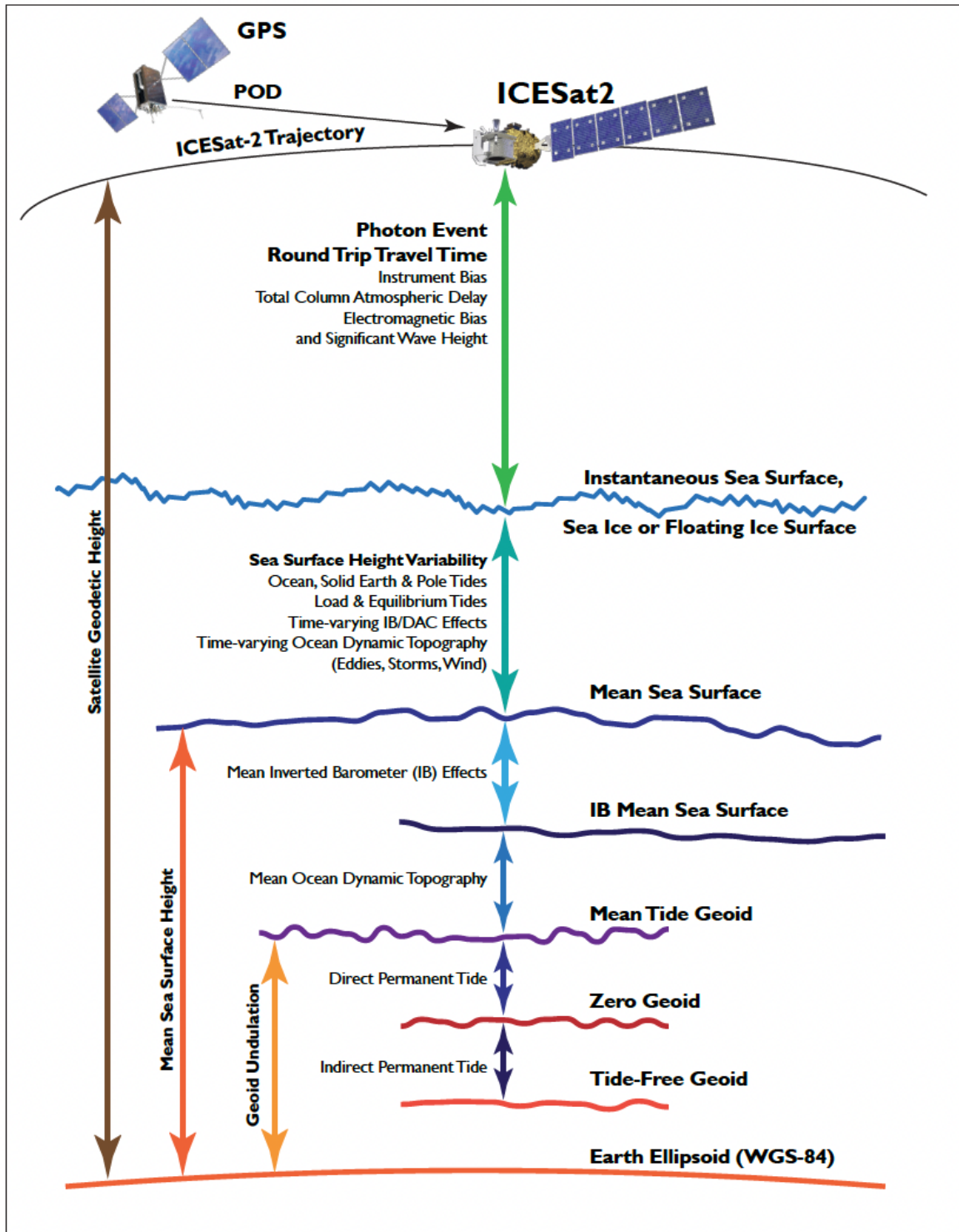


Figure 2. Geophysical corrections used in satellite altimetry. Taken from *ICESat-2 Data Comparison User's Guide for Rel006* available on the ATL03 data set landing page.

Table 1. Geophysical Corrections Applied to ICESat-2 Products

ICESat-2 Products by Surface Type	Geophysical Corrections <sup>1</sup>
Photon-level product (ATL03) (i.e., corrections applicable across all surface types)	Ocean loading Solid Earth tide Solid Earth pole tide Ocean pole tide Total column atmospheric range-delay
Land Ice, Land, and Inland Water (ATL06, ATL08, and ATL13)	<i>No corrections beyond ATL03</i>
Sea Ice (ATL07 and ATL10)	Referenced to mean sea surface Ocean tide Long period equilibrium ocean tide Inverted barometer (IB)
Ocean (ATL12)	Ocean tide Long period equilibrium ocean tide

<sup>1</sup>For details, see Section 5 of the *ICESat-2 Data Comparison User's Guide for Rel006* available on the ATL03 data set landing page.

### 1.2.3 File Contents

ATL06 data are provided as granules (files) that span about 1/14<sup>th</sup> of an orbit. Granule boundaries are delineated by lines of latitude that define 14 regions, numbered from 01–14, as shown in Figure 3.

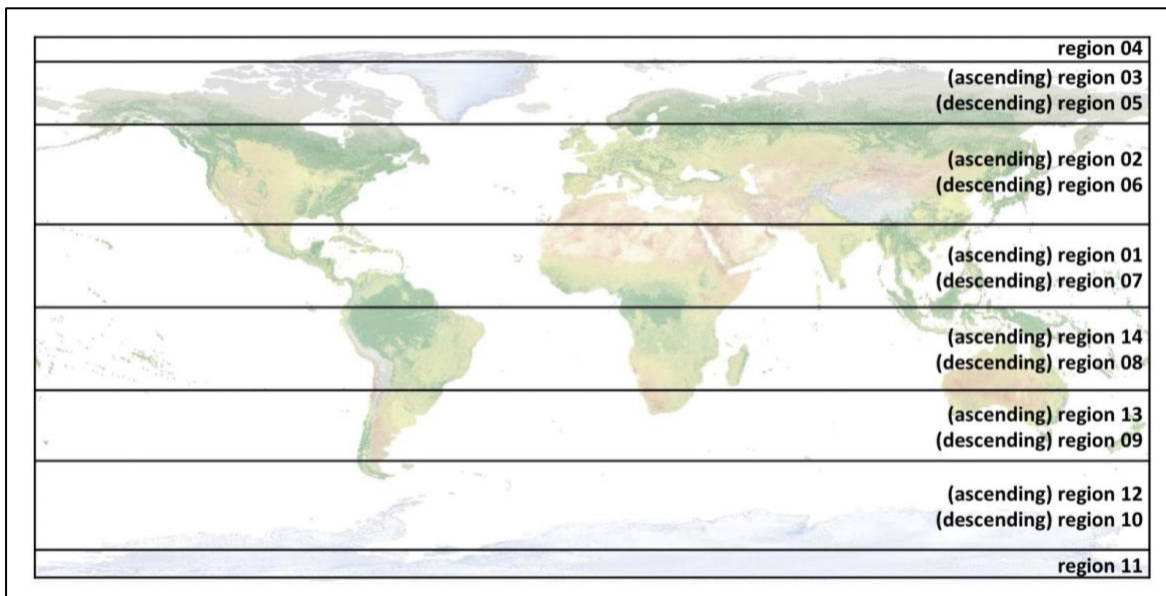


Figure 3. ATL06 region/granule boundaries.

The following table lists latitude bounds and region numbers for all 14 granule regions:

Table 2. ATLAS/ICESat-2 Granule Boundaries and Region Numbers

Region #	Latitude Bounds	Region #	Latitude Bounds
01	Equator → 27° N (ascending)	08	Equator → 27° S (descending)
02	27° N → 59.5° N (ascending)	09	27° S → 50° S (descending)
03	59.5° N → 80° N (ascending)	10	50° S → 79° S (descending)
04	80° N (ascending) → 80° N (descending)	11	79° S (descending) → 79° S (ascending)
05	80° N → 59.5° N (descending)	12	79° S → 50° S (ascending)
06	59.5° N → 27° N (descending)	13	50° S → 27° S (ascending)
07	27° N (descending) → Equator	14	27° S → Equator (ascending)

Note that the Land Ice Height product does not produce data granules for orbital segments that span open ocean only (i.e., do not cross a land surface).

### 1.2.4 Data Groups

Within data granules, similar variables such as science data, instrument parameters, altimetry data, and metadata are grouped together according to the HDF model and organized within the following top-level groups:

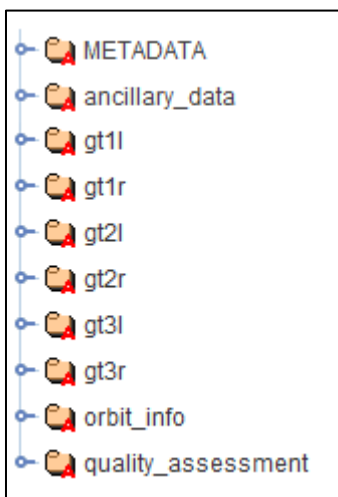


Figure 4. ATL06 data groups shown in HDFView.

The following sections summarize the contents of the data groups and certain parameters of interest. Data groups are described in detail in "Section 4 | ATL06 Data Product Description" in the ATBD for ATL06. A complete list of parameters is available in the ATL06 Data Dictionary.

#### 1.2.4.1 METADATA

ISO19115 structured metadata with sufficient content to generate the required geospatial metadata.

#### 1.2.4.2 ancillary\_data

Ancillary information such as product and instrument characteristics and/or processing constants. Data in this group pertain to the granule in its entirety.

#### 1.2.4.3 gt1l–gt3r

Each ground track group (six in all) contains three subgroups:

- **land\_ice\_segments:** contains primary ATL06 derived parameters, e.g., land-ice height (`h_li`), latitude, longitude, standard error, and quality measures. Heights represent the mean surface height, averaged along 40 m segments of ground track spaced 20 m apart, for each of ATLAS's six beams. Data are only provided for segment pairs for which at least one beam has a valid land-ice height measurement. Each reported height has a corresponding segment ID (stored in `segment_ID`), which indicates the second of the two 20 m ATL03 segments used to generate the 40 m ATL06 height segment.
- **residual\_histogram:** contains histograms of the residuals between photon event heights and the least-squares fit segment heights. Histograms are provided at a 200 m along-track rate.
- **segment\_quality:** contains a record of the success/failure of the surface-finding strategies for every possible segment in the granule, plus locations of the reference points on the reference pair tracks. For segments with adequate data quality, this subgroup contains offsets into the data structures for the other groups that allow each segment to be efficiently located within the file. Data are spaced 20 m apart along-track.

#### 1.2.4.4 orbit\_info

Parameters that are constant for a granule, such as the RGT number and cycle, the spacecraft orientation, and various ATLAS parameters needed by higher-level data products.

#### 1.2.4.5 quality\_assessment

Contains quality assessment data, including QA counters and QA along-track and/or summary data, organized in `gt[x]` subgroups. For more information, see Section 4.0 | ATL06 Data Product Description in the ATL06 ATBD.

## 1.2.5 Naming Convention

Data files utilize the following naming convention:

ATL06\_[yyyymmdd][hhmmss]\_[ttttccss]\_[vvv\_rr].h5

Example:

ATL06\_20181014025137\_02360112\_006\_01.h5

The following table describes the file naming convention variables:

Table 3. File Naming Convention Variables and Descriptions

Variable	Description
ATL06	ATLAS/ICESat-2 L3A Land Ice Height product
yyyymmdd	Year, month, and day of data acquisition
hhmmss	Hour, minute, and second of data acquisition (UTC)
tttt	Reference Ground Track. The ICESat-2 mission has 1,387 RGTs, numbered from 0001 to 1387.
cc	Cycle number. Each of the 1,387 RGTs is targeted in the polar regions once every 91 days. The cycle number tracks the number of 91-day periods that have elapsed since ICESat-2 entered the science orbit.
ss	Orbital segment (region) number (see Figure 3). ATL06 data files cover approximately 1/14 <sup>th</sup> of an orbit. Orbital segment numbers range 01–14. Note: data files are not produced for orbital segments that cross open ocean only (i.e., do not cross a land surface). As such, some orbital segments will not be available.
vvv_vv	Version and revision number*

Note: \*From time to time, NSIDC receives reprocessed granules from our data provider. These granules have the same file name as the original (i.e., date, time, ground track, cycle, and segment number), but the revision number has been incremented. Although NSIDC deletes the superseded granule, the process can take several days. If you encounter multiple granules with the same file name, please use the granule with the highest revision number.

Each data file has a corresponding XML file that contains additional science metadata. XML metadata files have the same name as their corresponding .h5 file, but with .xml appended.

### 1.2.5.1 Browse File

Browse files are provided as JPGs that contain images designed to quickly assess the location and quality of each granule's data. Images include ground track location, land ice heights, number of photon events (PEs) used for each beam, and a summary plot that shows height quality and

potential problems. Browse files utilize the same naming convention as their corresponding data file but with "\_BRW" and descriptive keywords appended.

## 1.3 Spatial Information

### 1.3.1 Coverage

The ICESat-2 mission acquires data along 1,387 different RGTs. However, this product does not produce data granules for orbital segments that span open ocean only (i.e., do not cross a land surface). As such, some granules/orbital segments will not be available.

NOTE: Starting with Version 6, ATL06 data are being processed for all global land regions and not restricted to just land ice. However, data outside of polar regions have not been thoroughly evaluated and may contain errors. Refer to the ATL06 Known Issues document for more information on using this experimental data.

#### 1.3.1.1 Land Ice Mask

[Static surface masks](#) (land ice, sea ice, land, and ocean) are applied to ATL03 to reduce the volume of data that a surface-specific along-track data product is required to process. The [land ice surface mask](#) directs the ATL06 land ice algorithm to consider data from only those areas of interest.

### 1.3.2 Resolution

Land ice heights represent the mean land ice surface height averaged along 40 m segments of ground track and spaced 20 m apart.

### 1.3.3 Geolocation

Points on Earth are presented as geodetic latitude, longitude, and height above the ellipsoid using the WGS 84 geographic coordinate system (ITRF2014 reference frame). The following table contains details about WGS 84:

Table 4. Geolocation Details

<b>Geographic coordinate system</b>	WGS 84
<b>Projected coordinate system</b>	N/A
<b>Longitude of true origin</b>	Prime Meridian, Greenwich
<b>Latitude of true origin</b>	N/A
<b>Scale factor at longitude of true origin</b>	N/A

<b>Datum</b>	WGS 84
<b>Ellipsoid/spheroid</b>	WGS 84
<b>Units</b>	degree
<b>False easting</b>	N/A
<b>False northing</b>	N/A
<b>EPSG code</b>	4326
<b>PROJ4 string</b>	+proj=longlat +datum=WGS84 +no_defs
<b>Reference</b>	<a href="https://epsg.io/4326">https://epsg.io/4326</a>

For information about ITRF2014, see the International Terrestrial Reference Frame | [ITRF2014 webpage](#).

## 1.4 Temporal Information

---

### 1.4.1 Coverage

14 October 2018 to 2 March 2025

Note that satellite maneuvers, data downlink issues, and other events can introduce data gaps into the ICESat-2 suite of products. As ATL03 acts as the bridge between the lower level, instrumentation-specific data and the higher-level products. On the data set landing page, users can download and consult a regularly updated [list of ATL03 data gaps](#) (.xlsx).

### 1.4.2 Resolution

Each of ICESat-2's 1,387 RGTs is targeted in the polar regions once every 91 days (i.e., the satellite has a 91-day repeat cycle).

## 2 DATA ACQUISITION AND PROCESSING

### 2.1 Background

---

ATL06 height estimates are derived from geolocated, time-tagged photon heights plus other parameters passed to ATL06 by the ATLAS/ICESat-2 L2A Global Geolocated Photon Data (ATL03) product. Figure illustrates the suite of ICESat-2 data products and their connections:

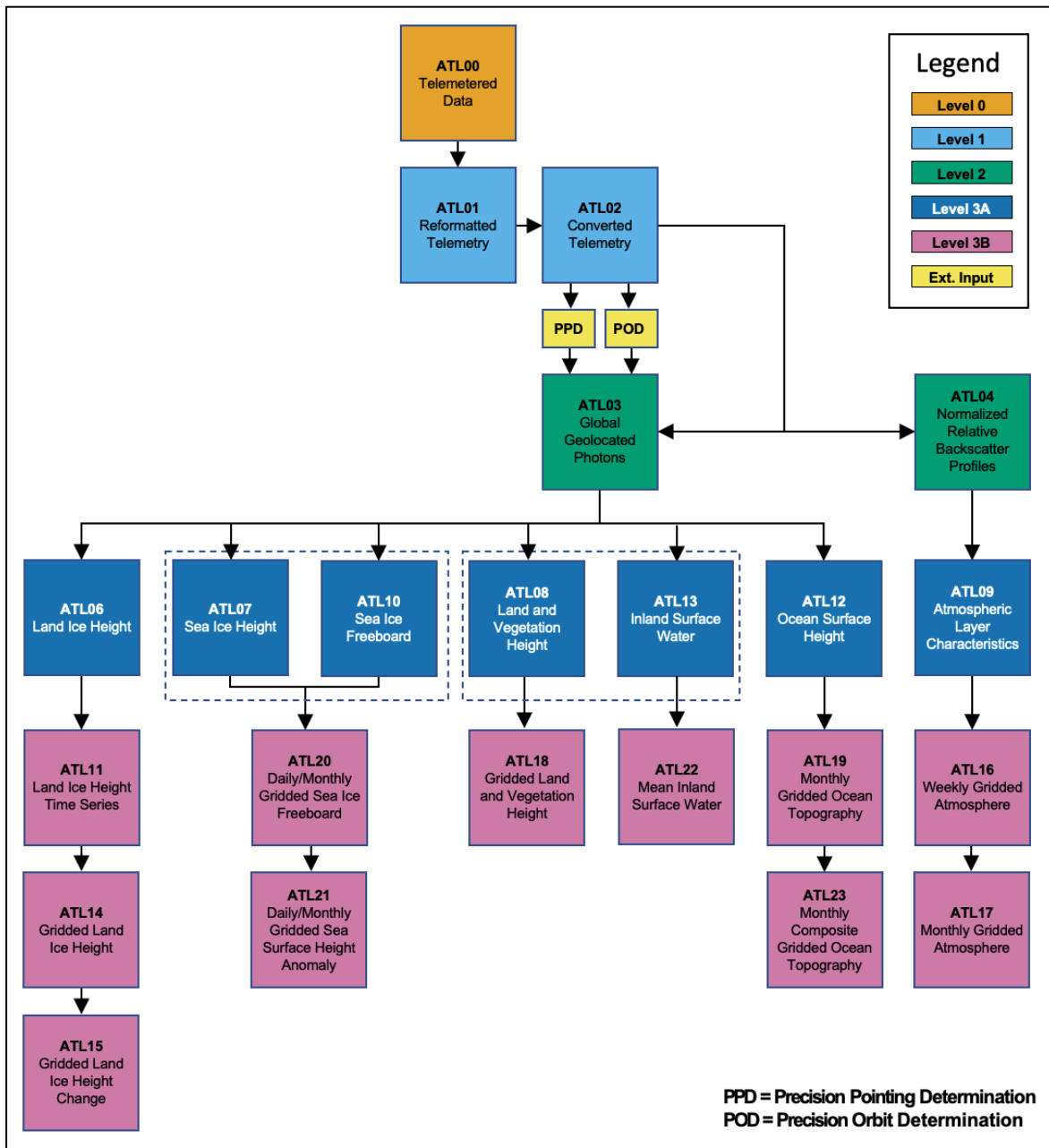


Figure 5. Schematic of the ICESat-2 data processing flow. The ATL01 algorithm reformats and unpacks the Level-0 data and converts it into engineering units. ATL02 processing converts ATL01 data to science units and applies instrument corrections. The Precision Pointing Determination (PPD) and Precision Orbit Determination (POD) solutions compute the pointing vector and position of the ICESat-2 observatory as a function of time.

## 2.2 Acquisition

The ATLAS instrument on ICESat-2 determines the range between the satellite and Earth’s surface by measuring the two-way time delay of short pulses of laser light that it transmits in six beams. ATLAS pulses are short—about 1.6 ns—and are transmitted every 0.1 ms (10 kHz). As the satellite

travels along its orbit, this fast repetition yields spots whose centers are separated by about 0.7 m in the along-track direction. Each pulse illuminates an approximately circular area on the ground about 14 m in diameter. ATLAS's strong beams generate at most 12 reflected photons from each transmitted pulse. Great care is taken to detect only photons with the same wavelength as the transmitted laser pulse and to limit the field of view of the detectors to a region that is just slightly larger than the illuminated spot. As such, ground-return PEs are clustered in time and may readily be distinguished from solar, background PEs, which are distributed evenly in time and arrive much less frequently.

## 2.3 Processing

---

The following section summarizes the approach used to generate the ATL06 data product. For a more complete description, consult the ATL06 ATBD.

ATL06 processing computes land ice surface heights and stores them by ground track so that subsequent measurements on the same reference pair track (RPT) can be easily compared. It also uses information from each strong/weak beam pair to estimate across-track slope. Additional parameters are also provided that indicate the quality of the surface-height estimates and the signal and noise levels associated with the measurement. The heights represent the mean surface height averaged along 40 m segments of ground track, spaced 20 m apart, for each of ATLAS's six beams. Segments within adjacent beams are aligned to facilitate estimation of the across-track surface slope. Segments are also aligned from orbit to orbit so that height estimates in subsequent repeat tracks lie at nearly the same location on the surface, thereby simplifying the task of computing height changes through time.

The algorithm utilizes an iterative process to select a small surface window that includes the majority of the signal PEs with as few as background PEs as possible. The surface height is then expressed as the median of the PE heights within the surface window, because the median is less sensitive to sampling error for distributions that contain a statistically uniform, background component. To estimate the spread of a distribution of PE heights, the algorithm uses the Robust Dispersion Estimator, which is equal to half the difference between the 16th and the 84th percentiles of a distribution. For Gaussian-distributed data, this statistic is approximately equal to the standard deviation, and for data containing a mixture of a large fraction of signal and a small fraction of noise, it provides an estimate of the spread of the signal that is relatively insensitive to the noise.

Land ice height is defined as the estimated surface height of the segment center for each reference point, using median-based statistics. The algorithm calculates this as the sum of the least-squares height fit, the first-photon-bias median correction, and the pulse-truncation median correction.

Height increment values are provided with the product that allow removal of the correction and the calculation of the segment mean height and first-photon-bias and pulse-truncation corrections corresponding to the segment mean.

The following steps outline the procedure used to generate land ice surface heights for each along-track reference point:

1. All PEs are collected from the current cycle that fall into the along-track bin for the along-track point.
2. The initial height and along-track slope are estimated for each beam in the pair.
3. The heights and surface windows are iteratively refined for each beam in the pair.
4. Corrections for subsurface scattering, first-photon bias, median offsets, and error estimates are calculated for each beam based on the edited PEs.
5. The across-track slope is calculated.

For a complete description of the ATL06 height derivation theory and implementation, see Section 3 | Algorithm Theory: Derivation of ATL06 Land Ice Height Parameters in the ATL06 ATBD.

## 2.4 Quality, Errors, and Limitations

---

Errors in ATLAS land-ice products can come from a variety of sources:

1. Sampling error: ATLAS height estimates are based on a random sampling of the surface height distribution;
2. Background noise: Random-noise PEs are mixed with the signal PEs, so sampled PEs will include random outliers;
3. Complex topography: The along-track linear fit and across-track polynomial fit do not always resolve complex surface topography.
4. Misidentified PEs: The ATL03 product will not always identify the correct PEs as signal PEs;
5. First-photon bias: This is an error inherent to photon-counting detectors that results in a high bias in the mean detected PE height that depends on signal strength;
6. Atmospheric forward scattering: Photons traveling downward through a cloudy atmosphere may be scattered through small angles but still be reflected by the surface within the ATLAS field of view; these will be delayed, producing an apparently lower surface;
7. Subsurface scattering: Photons may be scattered many times within ice or snow before returning to the detector; these will be delayed, producing a surface estimate with a low bias.

Each of these errors are treated differently during the ATL06 processing:

- 1 and 2 (above) are treated as random errors and their effects are quantified in the error estimates associated with the product.
- 3 and 4 will produce relatively large errors that will need to be addressed with consistency checks when higher-level products are generated.
- 5 will be corrected routinely during ATL06 processing.

- 6 and 7 are not quantified in ATL06. They require information about cloud structure and ice-surface conditions that are not available when ATL06 is processed. Correcting for these errors remains an active avenue of research.

Potential error sources and mitigation strategies are detailed in Section 2.3 | Potential Errors and Section 3.6 | Signal, Noise, and Error Estimates in the ATL06 ATBD.

### 3 VERSION HISTORY

A summary of the version history is provided in Table 5.

Table 5. Version History Summary

Version	Release Date	Description
V1	May 2019	Initial release
V2	October 2019	Refer to V2 User Guide
V3	May 2020	Refer to V3 User Guide
V4	April 2021	Refer to V4 User Guide
V5	November 2021	Refer to V5 User Guide
V6	May 2023	<ul style="list-style-type: none"> <li>• <b>Processing data for all global land regions.</b> These data are considered experimental, and no quality checks are being performed for the data outside of the polar regions.</li> <li>• <b>Dynamically computing the radial component of geolocation uncertainty (<math>\sigma_{geo\_r}</math>).</b> Previously, this value was fixed. The uncertainty is calculated for ATL03 (<math>\sigma_h</math>) and the value is passed through to ATL06 (<math>\sigma_{geo\_r}</math>). Values for the horizontal geolocation uncertainties (<math>\sigma_{geo\_at}</math> and <math>\sigma_{geo\_xt}</math>) remain at fixed, pessimistic values of 5 m.</li> </ul>
V6.1	May 2024	Data from 13 November 2022 to 26 October 2023 were reprocessed using ITRF2014 (replacing ITRF2020) for consistency across the entire data set.
V6.1	March 2026	Removed data access for v6.1. Data coverage was 14 Oct 2018 to 2 Mar 2025.

### 4 REFERENCES

#### 4.1 References

Bamber, J. L., Gomez-Dans, J. L., & Griggs, J. A. (2009). A new 1 km digital elevation model of the Antarctic derived from combined satellite radar and laser data - Part 1: Data and methods. *Cryosphere*, 3(1), 101–111. <https://doi.org/10.5194/tc-3-101-2009>

Menke, W. (1989). *Geophysical data analysis: discrete inverse theory*. Academic Press.

Scambos, T. A., Haran, T. M., Fahnestock, M. A., Painter, T. H., & Bohlander, J. (2007). MODIS-based Mosaic of Antarctica (MOA) data sets: Continent-wide surface morphology and snow grain size. *Remote Sensing of Environment*, 111(2–3), 242–257.

<https://doi.org/10.1016/j.rse.2006.12.020>

Warren, S. G., Brandt, R. E., & Grenfell, T. C. (2006). Visible and near-ultraviolet absorption spectrum of ice from transmission of solar radiation into snow. *Applied Optics*, 45(21), 5320–5334.

<https://doi.org/10.1364/AO.45.005320>

Yang, Y., Marshak, A., Palm, S. P., Varnai, T., & Wiscombe, W. J. (2011). Cloud Impact on Surface Altimetry From a Spaceborne 532-nm Micropulse Photon-Counting Lidar: System Modeling for Cloudy and Clear Atmospheres. *IEEE Transactions on Geoscience and Remote Sensing*, 49(12), 4910–4919.

<https://doi.org/10.1109/TGRS.2011.2153860>

Yang, Y., Marshak, A., Palm, S. P., Wang, Z., & Schaaf, C. (2013). Assessment of Cloud Screening With Apparent Surface Reflectance in Support of the ICESat-2 Mission. *IEEE Transactions on Geoscience and Remote Sensing*, 51(2), 1037–1045.

<https://doi.org/10.1109/TGRS.2012.2204066>

Yi, D. H., & Bentley, C. R. (1999). Geoscience Laser Altimeter System waveform simulation and its applications. *Annals of Glaciology*, 29, 279–285. <https://doi.org/10.3189/172756499781821580>

## 5 DOCUMENT INFORMATION

### 5.1 Publication Date

---

May 2023

### 5.2 Date Last Updated

---

March 2026